IEEE Access
Multidisciplinary | Rapid Review | Open Access Journal

Received March 18, 2018, accepted April 18, 2018, date of publication May 1, 2018, date of current version May 24, 2018.

Digital Object Identifier 10.1109/ACCESS.2018.2831911

A UAV Detection Algorithm Based on an Artificial Neural Network

HAO ZHANG[1,2], (Senior Member, IEEE), CONGHUI CAO[1], LINGWEI XU[3], AND T. AARON GULLIVER[2], (Senior Member, IEEE)

[1]Department of Electrical Engineering, Ocean University of China, Qingdao 266100, China
[2]Department of Electrical and Computer Engineering, University of Victoria, Victoria, BC V8W 2Y2, Canada
[3]Department of Information Science and Technology, Qingdao University of Science & Technology, Qingdao 266061, China

Corresponding authors: Conghui Cao (caoconghui2008@163.com) and Lingwei Xu (gaomilaojia2009@163.com)

This work was supported in part by the National Natural Science Foundation of China under Grant 61701462 and Grant 41527901, in part by the Qingdao National Laboratory for Marine Science and Technology under Grant 2017ASKJ01, in part by the Qingdao Science and Technology Plan under Grant 17-1-1-7-jch, in part by the Fundamental Research Funds for the Central Universities under Grant 201713018, in part by the Shandong Province Natural Science Foundation under Grant ZR2017BF023, in part by the China Postdoctoral Science Foundation funded project under Grant 2017M612223, and in part by the Shandong Province Postdoctoral Innovation Project under Grant 201703032.

ABSTRACT This paper presents an artificial neural network (ANN)-based detection algorithm for an unmanned aerial vehicle (UAV). The slope, kurtosis, and skewness of the signal received from the UAV are employed in this algorithm. The training of the three corresponding feature matrices is done using UAV, and non-UAV signals can be classified effectively for the UAV sensor network based on ANN. Outdoor data over a bridge in the Jimo District, Qingdao, and indoor data from a research laboratory are used for system training and evaluation. The results obtained show that the proposed detection algorithm based on an ANN outperforms methods based on the slope, kurtosis, and skewness of the received signal in terms of the error rate. The recognition rate with the proposed algorithm is greater than 82% within a distance of 3 km, which is better than other UAV detection methods such as active radar, acoustic, and visual recognition.

INDEX TERMS Unmanned aerial vehicle (UAV), wireless sensor networks, artificial neural network (ANN), signal detection, slope, kurtosis, skewness.

I. INTRODUCTION

In recent years, there has been significant research on wireless sensor networks (WSNs) [1]–[4]. Unmanned aerial vehicle (UAV) sensor networks are becoming important for both civilian and military applications because of their low cost, coverage, and agility and the availability of small-scale sensors [5]. According to BI Intelligence, the global UAV market is expected to grow at a compound annual growth rate (CAGR) of 19% between 2015 and 2020, with the military market growing by 5%. This because UAVs are now widely used in the fields of mapping, military operations, precision agriculture, aerial photography, environmental monitoring, search and rescue, and video recording [6]. However, beyond these applications, there have been problems such as a UAV crashing at the White House and another interrupting a US Open tennis match. A UAV collided with a Lufthansa jet near Los Angeles International Airport (LAX) on March 29, 2016, which raises concerns regarding the safety of government buildings, air traffic and other facilities [7]. Small UAVs can also be used to invade the privacy of people. Shooting a UAV is the most direct approach to dealing with a threat. In [8] and [9], a genetic algorithm (GA) was used for UAV jamming. Jamming the GPS or radio signals was considered in [10] to disable a UAV without damaging it [10]. However, these methods are based on the assumption that the UAV has been detected and its location is known.

The urgent need for human safety, security, and privacy has made UAV detection a research focus. Many detection algorithms have been proposed such as active radar probe, acoustic recognition, infrared spectrum identification, visual recognition and radio frequency signal detection [7], [11]–[15]. In [11], an active radar system using a frequency modulated signal was proposed to detect a small UAV within a distance of 500 m. A calibrated radar cross section (RCS) was used in [12] to recognize a UAV within a range of 2 km regardless of the flight pattern [12]. A regularized 2-D complex-log-Fourier transform algorithm was considered in [13] to extract spectrogram features to identify the Doppler signature of a UAV. Space-variant resolution (SVR) and log-polar transformations (LPTs) were employed in [14] to identify UAVs even

with scale and rotational changes [14]. However, beyond a distance of 1.5 km detection system have difficulty distinguishing between birds and UAVs [13], [16]. Beamforming with an acoustic array was considered in [15] to locate and track UAVs, but its effective range is less than 300 m. In [7], a passive detection algorithm was employed to extract the low-frequency communication signals between the UAV and controller. In this paper, the statistical features of the corresponding high-frequency signals.

Many characteristics have been employed in the statistical analysis of signals such as power quality, brain-computer interface, and energy [17]–[20]. Most are closely related to the slope, skewness, and kurtosis of the signals. For example, the power quality was examined and the disturbances classified in [17] using the skewness, kurtosis and Shannon entropy of the voltage. The initial dips in a brain-computer interface were obtained in [18] by considering five features: signal mean, peak value, signal slope, skewness, and kurtosis. Thus, it can be concluded that the statistical features of a signal should prove useful in detection UAVs, even in complex environments.

As we all know, common nonlinear-system-modeling methods include artificial neural network (ANN), support vector machine (SVM), k-nearest neighbor (KNN), GA, naive Bayes classifier (NBC), decision tree, Kalman filter, etc [21]–[23]. GA has better performance compared with ANN but it requires higher receiver complexity. SVM has a little advantage on the recognition rate than ANN, but it is difficult to implement training and classification for a large number samples in the large-scale and long-time UAV detection. KNN usually tends to be a poor robustness in nonlinear recognition because of its lazy learning method and low prediction speed. NBC and decision tree only apply to the system with the assumption of characteristics being independent of each other, which is not suitable for the UAV signal involved in this paper. While ANN is a popular self-learning method for characterizing complex relationships to achieve robust nonlinear approximations [24]. They have been widely used in the field of statistical signal processing. It has advantages of simple structure, strong learning ability, high accuracy, great approximation ability and good fault tolerance for the noise, which is very suitable for UAV detection requirement. With this approach, it is important that the ANN is trained appropriately to obtain suitable weights in the layers. Then an accurate target classification and recognition system for UAV signal can be developed.

In this paper, feature extraction and classification from radio frequency (RF) signals using an ANN is considered for UAV detection. The main innovations and contributions are as follows.

Different from other articles of UAV detection, the UAV communication signal is used as an identification marker for the first time in this paper. Besides, UAV signal features in the frequency domain are extracted innovatively, which includes the slope, kurtosis, and skewness. Meanwhile, in this paper, the first combination of improved features and ANN algorithm is achieved to classify the received signals as UAV or non-UAV. In addition, a lot of real data is collected from indoor and outdoor environments for the first time to test the effectiveness of the proposed algorithm. By the comparison of experimental results, it is proved that the proposed method of this paper is more suitable for UAV detection than other means.

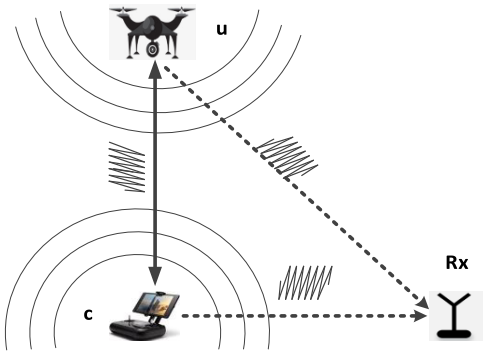

FIGURE 1. System model.

The remainder of this paper is organized as follows. The UAV system model and the noise reduction method are introduced in Section II. Section III considers the statistical characteristics of UAV communication signals. In Section IV, three characteristics are improved for identifying a UAV, and an ANN-based algorithm to recognize UAV RF signals is proposed. Section V presents performance results using data from both indoor and outdoor environments which confirm the effectiveness of the proposed detection strategy. Finally, some concluding remarks are given in Section VI.

II. SYSTEM MODEL

We consider a UAV u and a controller c which emit RF signals when they communicate with each other, and an RF signal receiver Rx. Fig. 1 shows the system model. Most UAVs operate in the frequency band 2.4 – 2.4835 GHz using frequency hop spread spectrum for image transmission and flight control [25]. The UAV communication signals conform to the IEEE 802.11 standard [26]. The Phantom 4 Pro UAV and controller manufactured by DJ-Innovations is an example of a typical system and are employed here.

A dataset was obtained with a distance between u and Rx of 2.5 km and a distance between c and Rx of 2.5 km. The received power is $y(f), f = 2.4 \times 10^9, \ldots, 2.5 \times 10^9$ Hz with a total of 5120 points was collected by the Rx with a frequency spacing of fw $=$ 19.53 kHz. Fig. 2(a) shows the received signal power in dBm.

Empirical mode decomposition (EMD) is used to remove noise from the UAV signal [27], [28]. EMD decomposes a signal into multiple signal-frequency intrinsic mode functions (IMF) and a residual signal which can be expressed as

$$y_f = \sum_{i=1}^{n} imf_i(f) + r_n(f) \tag{1}$$

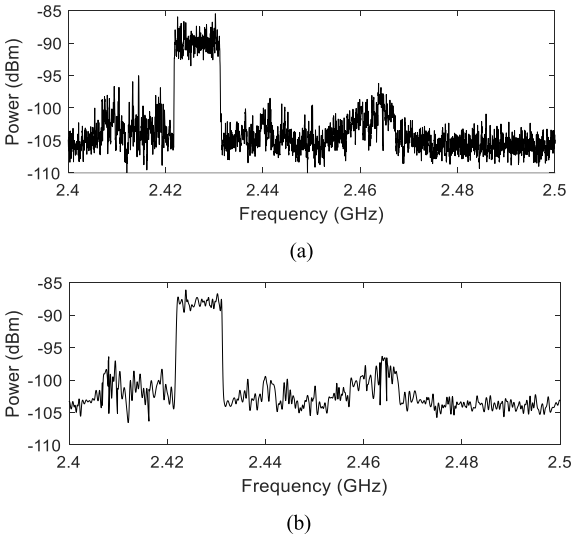

FIGURE 2. EMD denoising of the UAV signal. (a) The original UAV communication signal. (b) The UAV communication signal after EMD.

where imf_i denotes ith IMF and r_n is the residual wave after the nth decomposition. The resulting sequence after discarding the first three IMFs is

$$\dot{y}_f = \sum_{i=4}^{n} imf_i(f) + r_n(f) \tag{2}$$

and is shown in Fig. 2(b). This shows that the communication signal has a bandwidth of approximately 9.8 MHz when the UAV is transmitting images. Because of the large distance between the Rx and u in a real outdoor environment, the channel between u and Rx is typically line of sight (LOS) while the channel between c and Rx is usually non line of sight (NLOS). An indoor environment is more complex due to multipath effects and interference from other wireless signals. This paper considers the detection of UAV and non-UAV signals in indoor and outdoor environments. A non-UAV signal here refers to noise (no UAV signal present).

III. STATISTICAL FEATURES OF THE UAV COMMUNICATION SIGNAL

In this section, the kurtosis, skewness, and slope of the UAV signal are investigated. According to the features of the UAV signal, a sliding window of width 9.77 MHz is used for the kurtosis and skewness and a window of width 488.3 kHz for the slope.

A. SLOPE OF THE UAV COMMUNICATION SIGNAL

Slope denotes the inclination of a straight line or the tangent to a curve [19]. Here, a set of data from the test includes 5120 sample points and is distributed in the 2.4-2.5 GHz band evenly. We choose 488.3 kHz also corresponding to N_a sample points as a sliding window to fit a straight line and obtain the slope. The slope of the kth window is given by (3), as shown at the top of the next page where $N_a = 25$ and

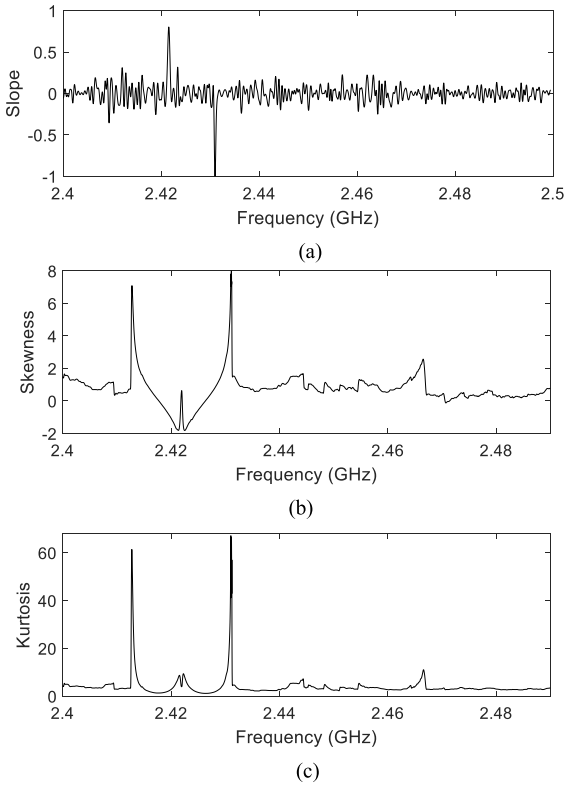

FIGURE 3. Features of the UAV communication signal. (a) Normalized slope of the UAV communication signal. (b) Skewness of the UAV communication signal. (c) Kurtosis of the UAV communication signal.

$f_k = 2.4 \times 10^9 + (k-1) \times f_w$ is the starting frequency of the kth window, $k = 1, 2, \ldots, (2.5-2.4) \times 10^9/\mathrm{f_w} - N_a + 1$. The resulting slope values are shown in Fig. 3(a). This indicates there is a large slope at the rising edge and a small slope at the falling edge of the UAV signal.

B. SKEWNESS OF THE UAV COMMUNICATION SIGNAL

The skewness describes the asymmetry of a signal, and the skewness of the symmetry distribution is zero [19]. Here we choose 9.77 MHz also corresponding to N_b sample points as a sliding window to compute the skewness. The frequency interval of sliding is f_w. Further, skewness of the kth window can be given by

$$S^k = \frac{1}{\sigma^3 (N_b - 1)} \sum_{f=f^k}^{f^k + (N_b-1) \times f_w} \left(y_f - \bar{y}_f\right)^3 \tag{4}$$

where N_b equals 500, σ and $\bar{y}_f$ are the variance and the mean of sample points in the window respectively. When $S^k > 0$, the sliding window has a large right tail and biases to the left. When $S^k < 0$, the sliding window has a large left tail and biases to the right. Along with the sliding of the window, we can obtain all the skewness values for all frequency positions in Fig. 3(b). As we can see that the skewness of the square wave for the UAV RF signal is close to 0.

$$L^k = \frac{N_a \times \sum_{f=f^k}^{f^k+(N_a-1)\times f_w} f\dot{y}_f - \left(\sum_{f=f^k}^{f^k+(N_a-1)\times f_w} f\right)\left(\sum_{f=f^k}^{f^k+(N_a-1)\times f_w} \dot{y}_f\right)}{N_a \times \left(\sum_{f=f^k}^{f^k+(N_a-1)\times f_w} f^2\right) - \left(\sum_{f=f^k}^{f^k+(N_a-1)\times f_w} f\right)^2} \tag{3}$$

C. KURTOSIS OF THE UAV COMMUNICATION SIGNAL

The kurtosis can measure the peakedness and the tail heaviness of distribution simultaneously [20]. Just as the kurtosis value for the normal distribution equals three. Here we also choose 9.77 MHz corresponding to N_b sample points as a sliding window to compute the kurtosis which can be given by

$$K^k = \frac{1}{\sigma^4 (N_b - 1)} \sum_{f=f^k}^{f^k+(N_b-1)\times f_w} \left(y_f - \bar{y}_f\right)^4 \tag{5}$$

where k refers to the kth window, σ and $\bar{y}_f$ are the variance and the mean of sample points in the kth window respectively, the frequency interval of sliding also is f_w.

When $K^k > 0$, the sliding window meets the super-Gaussian distribution and has a large tail. When $K^k = 0$, it obeys the distribution of Gaussian. Along with the sliding of the window, we can obtain all the kurtosis values for all frequency positions in Fig. 3(c). As we can see that the kurtosis of the square wave for the UAV RF signal is in the range of 0 to 2.5.

IV. ANN BASED DETECTION OF THE UAV SIGNAL

A UAV signal recognition method does not currently exist in the literature. Thus, a detection technique is developed here which is based on modifications of the three features described above. In this section, modifications of the slope L^k, skewness S^k, and kurtosis K^k are employed to develop an algorithm to detect UAV signals. An ANN is used to establish the relationship between the characteristic matrix and the classification vector to determine if a UAV signal exists in the received data.

A. IMPROVED SLOPE FOR UAV SIGNAL DETECTION

The slope indicates the presence of a UAV when it is greater than a positive threshold in one position and less than a negative threshold in the another position with the number of samples between these positions is in the range $9.18 \times 10^6/f_w$ to $10.35 \times 10^6/f_w$. To improve detection, the improved slope $\dot{F}$ is proposed which is expressed in (6). $PST = 0.68$ is the positive threshold, $NST = -0.68$ is the negative threshold, L^p and L^q are the slopes in the pth and qth windows, respectively, P_a and Q_b are the window positions, A and B is the number of window positions meeting the condition, and F_{ab} is the interval between P_a and Q_b. $\dot{F}$ in the range 470 to 530 indicates a UAV signal is present, otherwise the signal is not present.

$$\dot{F} = \begin{cases} \max(F_{ab})\ s.t.\ 9.18\times10^6/f_w \le F_{ab} \le 10.35\times10^6/f_w, \\ \quad F_{ab} = P_a - Q_b, \\ \quad P_a \in \mathbf{P}, a = 1,\ldots,A, Q_b \in \mathbf{Q}, b = 1,\ldots,B, \\ \quad \left(\mathbf{P} = p\,|_{(\exists L^p \le NST)}\right) \cap \left(\mathbf{Q} = q\,|_{(\exists L^q \ge PST)}\right), \\ \quad 1 \le q \le p \le (2.5-2.4)\times10^9/f_w - N_a + 1 \\ P - Q\ s.t.\ P = p\,|_{\min(L^p)}, Q = q\,|_{\max(L^q)}, \\ \left(\begin{array}{l} \overline{9.18\times10^6/f_w \le F_{ab} \le 10.35\times10^6/f_w,} \\ F_{ab} = P_a - Q_b, \\ P_a \in \mathbf{P}, a = 1,\ldots,A, Q_b \in \mathbf{Q}, b = 1,\ldots,B \end{array}\right) \\ \quad \cap \left(\mathbf{P} = p\,|_{(\exists L^p \le NST)}\right) \cap \left(\mathbf{Q} = q\,|_{(\exists L^q \ge PST)}\right) \\ \quad \cup \left(\overline{\left(\mathbf{P} = p\,|_{(\exists L^p \le NST)}\right) \cap \left(\mathbf{Q} = q\,|_{(\exists L^q \ge PST)}\right)}\right), \\ \quad 1 \le q \le p \le (2.5-2.4)\times10^9/f_w - N_a + 1 \end{cases} \tag{6}$$

B. IMPROVED SKEWNESS OF THE UAV SIGNAL

A UAV is assumed to exist if there is a position where the skewness of the corresponding window is close to 0. Thus, the improved skewness used in the detection algorithm is expressed as

$$\dot{S} = \min(|S^k|), \quad k = 1,\ldots,(2.5-2.4)\times10^9/f_w - N_b + 1 \tag{7}$$

Then $\dot{S}$ lower than 0.0025 indicates a UAV signal is present, otherwise the signal is not present.

C. IMPROVED KURTOSIS OF THE UAV SIGNAL

A UAV is assumed to exist when a position with kurtosis of the corresponding window is in the range 0 to 2.5. Thus, the kurtosis feature used in the detection algorithm is given by

$$\dot{K} = \max(2.5 - K^k), \quad k = 1,\ldots,(2.5-2.4)\times10^9/f_w - N_b + 1 \tag{8}$$

Then $\dot{K}$ greater than 0 indicates a UAV signal is present, otherwise the signal is not present.

D. THE ANN BASED UAV DETECTION ALGORITHM

It is important to choose an ANN with appropriate features to reduce the computational complexity and increase the recognition rate [18]. The classification value λ_i for the ith set of data may equal 1 or 2 belonging to the UAV class or the

non-UAV class respectively. The characteristic vector for the ith set of data is described as

$$\mathbf{h}_i = [\dot{F}_i, \dot{S}_i, \dot{K}_i], \quad i = 1, \ldots, N \tag{9}$$

where $\dot{F}_i$, $\dot{S}_i$ and $\dot{K}_i$ are the improved slope, improved skewness and improved kurtosis for the ith dataset, respectively.

In fact, back propagation neural network (BPNN) belongs to ANN and can approximate any nonlinear continuous function with arbitrary precision using a three-layer neural network, which makes it particularly suitable for solving UAV detection problem with complex internal mechanisms [29]. Meanwhile, in order to improve the BPNN, Levenberg-Marquardt (LM) as training method is selected to accelerate convergence in this paper. Radical basis function neural network (RBFNN) also is an ANN type, possesses all the advantages of the ANN and is superior to BPNN in many aspects, but the structure of BPNN is simpler than that of RBFNN when solving UAV detection problem with the same accuracy requirement [30]. As a model of unsupervised learning, self-organizing mapping neural network (SOMNN) maps high dimensional data onto smaller dimension and keeps the topological features by the neighborhood function, but dead neurons may happen because that the input vector is too far to participate in learning. In addition, convolutional neural network (CNN) has better performance compared with BPNN but it requires higher receiver complexity.

Therefore, in order to simplify the receiver structure and achieve high recognition rate for UAV signal, BPNN is used to determine the relationship between the characteristic matrix $\mathbf{h}$ and the classification vector $\boldsymbol{\lambda}$ using the N sets of data. This network has an input layer, an output layer, and a hidden layer. This mapping g can be expressed as

$$\mathrm{g}{:}\mathbf{h} \rightarrow \boldsymbol{\lambda} \tag{10}$$

where $\mathbf{h} = [h_1, \ldots, h_N]'$ and $\boldsymbol{\lambda} = [\lambda_1, \ldots, \lambda_N]'$.

In order to reduce the computational complexity and improve performance, the network parameters are adjusted. The average mean squared error (MSE) was obtained after training with N groups of data 500 times with 2 to 50 neurons. The average MSE improves as N increases but the computational complexity also increases. By weighing the stability and convergence from multiple results of simulation test, we decide to make use of 18 neurons in hidden layer to train the data with the less average MSE finally. The number of iteration times is set to 500 in every training and the learning rate is set to 0.01. Furthermore, the LM algorithm is chosen as the fastest training algorithm combining the Newton method and Gradient descent method and the transfer function among layers is the log sigmoid function which can be given by

$$\log\mathrm{sig}(x) = \frac{1}{(1 + \exp(-x))} \tag{11}$$

Fig. 4 presents a flow chart of the UAV signal detection algorithm. As we can see that the training vectors in training procedures includes a classification vector $\boldsymbol{\lambda}$ with length of N and a feature matrix $\mathbf{h}$ with length $3N$. After training, a discriminant model is obtained. Then, in the test stage, by extracting the characteristic matrix from the testing samples to the model, their class will be evaluated. When $g(h_i) > 0.5$, the ith set of test data belongs to the UAV category, otherwise it belongs to the non-UAV category.

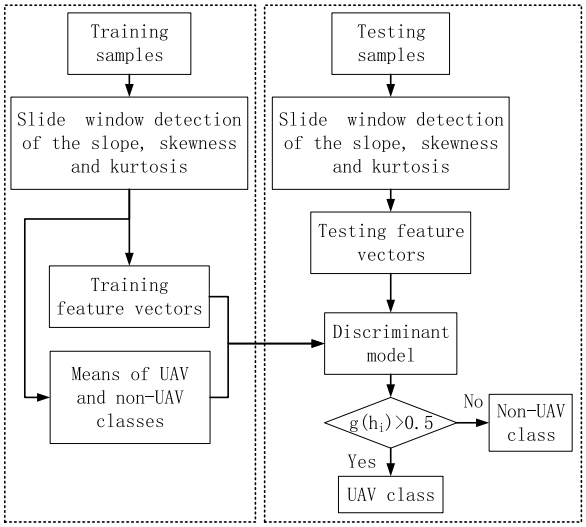

FIGURE 4. Flow chart of the UAV signal detection.

TABLE 1. Locations and corresponding feature values.

	Positions of u and c (m, m, m)	UAV			Non-UAV		
		$\dot{F}$	$\dot{S}$	$\dot{K}$	$\dot{F}$	$\dot{S}$	$\dot{K}$
Indoor	(0, 5, 3), (3, 0, 0)	528	6.916e-4	0.736	264	0.551	-0.943
	(0, 10, 3), (3, 0, 0)	517	1.490e-3	0.941	90	0.479	-1.343
	(0, 15, 3), (3, 0, 0)	509	2.412e-5	0.7828	1257	0.299	-1.238
Outdoor	(0, 5, 5), (5, 0, 0)	521	2.412e-4	0.8957	17	0.493	-0.855
	(0, 10, 10), (5, 0, 0)	511	1.913e-3	0.5591	181	0.541	-0.539
	(0, 20, 20), (5, 0, 0)	517	1.125e-3	0.8977	3595	0.484	-2.379
	(0, 500, 100), (5, 0, 0)	516	1.225e-4	0.7207	1039	0.256	-1.615
	(0, 1000, 100), (0, 1000, 0)	513	8.102e-4	0.6767	92	0.786	-1.747
	(0, 1500, 100), (0, 1500, 0)	510	1.447e-5	0.7325	2437	0.115	-0.623
	(0, 2000, 100), (0, 2000, 0)	529	1.023e-3	0.8749	673	0.613	-1.421
	(0, 2500, 100), (0, 2500, 0)	508	9.755e-4	0.9125	191	0.409	-2.057
	(0, 3000, 100), (0, 3000, 0)	525	7.654e-4	0.7396	348	0.577	-0.334

V. PERFORMANCE RESULTS

The proposed algorithm is evaluated in real indoor and outdoor environments. The indoor environment is a university laboratory with dimensions 10 m × 15 m × 5 m and the outdoor environment is over a bridge in the Jimo District, Qingdao, City Shandong Province, China with dimensions

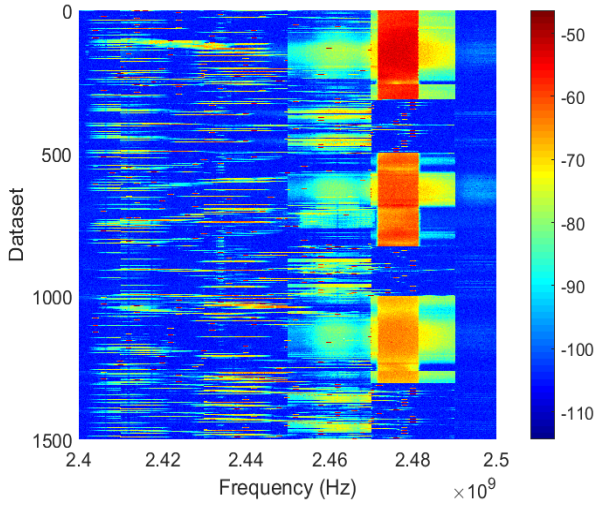

FIGURE 5. Training data in an indoor environment.

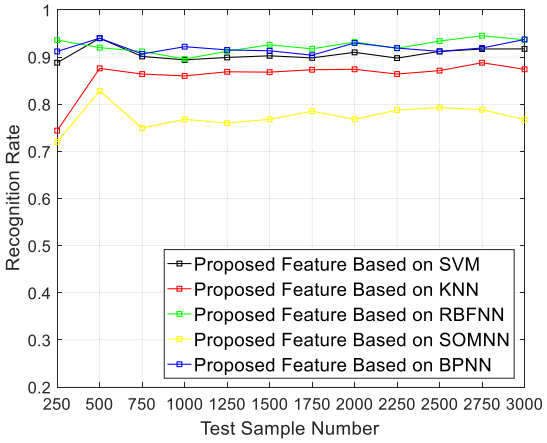

FIGURE 6. Recognition rate in an indoor environment for different modeling methods and number of samples.

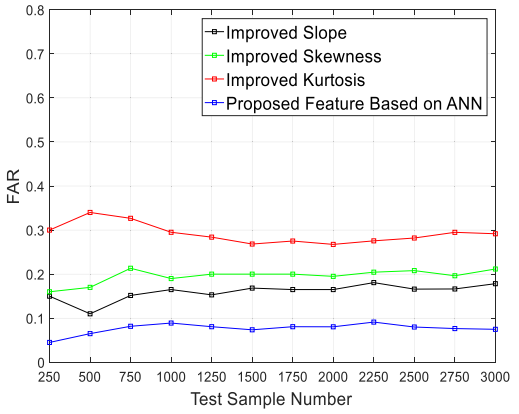

FIGURE 7. FAR with four feature detection algorithms in the indoor environment.

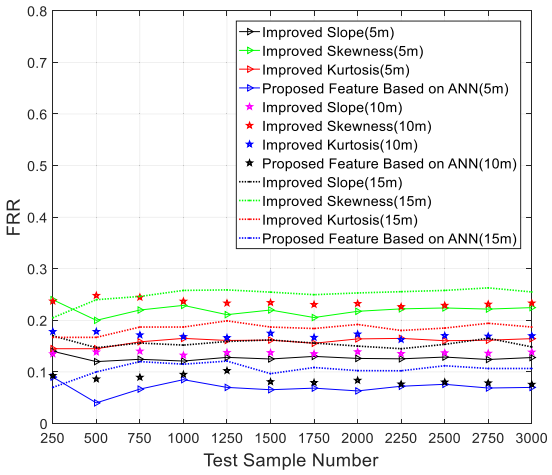

FIGURE 8. FRR of four feature detection methods in an indoor environment for different distances and number of samples.

1000 m × 4000 m × 200 m. The receiver Rx is located at position (0 m, 0 m, 0 m) and the UAV u and the controller c locations are given in Table I along with the corresponding values of $\dot{F}$, $\dot{S}$ and $\dot{K}$.

A. INDOOR UAV TEST

Part of indoor receiving data as the training data is shown in Fig. 5 with datasets of 1 to 500, 501 to 1000, and 1001 to 1500 correspond to the distance of 5 m, 10 m, and 15 m between Rx and u respectively. Obviously, the data of the front half for each distance belongs to the UAV class, while the data of the back half for each distance belongs to the non-UAV class. After training, a test model is formed to detect the RF signal of the UAV indoors.

Choosing a different number of samples from 250 to 3000 from all indoor samples randomly as test data, Fig. 6 shows the recognition rate using five nonlinear modeling methods in an indoor environment. The false acceptance rate (FAR) of different number of non-UAV category data with four feature detection algorithm is shown in Fig. 7. The false rejection rate (FRR) of UAV category data with the four techniques is given in Fig. 8 for the three distance of 5 m, 10 m and 15 m with a different number of samples from 250 to 3000. While Fig. 9 shows the recognition rate using proposed feature detection algorithm in indoor environment. FAR is defined as the percentage of non-UAV category signal being wrongly classified as UAV category. FRR is defined as the percentage of UAV category signal being wrongly classified as non-UAV category. Recognition rate is defined as the percentage of classifying UAV and non-UAV category signals correctly from different number of random data.

In Fig. 6, it is obvious that KNN and SOMNN have lower performance than other ways because of lazy learning method and forming dead neurons respectively. Besides, the recognition rate of SVM, RBFNN and BPNN are 0.8992, 0.9124, and 0.9152 respectively when the indoor test sample number is 1250. BPNN has better accuracy than SVM. Although the performance of BPNN is very similar to RBFNN, BPNN has a simpler structure than RBFNN. Therefore, BPNN we used

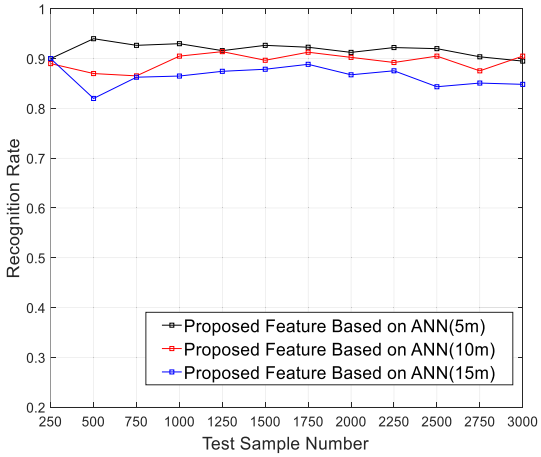

FIGURE 9. Recognition rate of our proposed feature at indoor different distances with different sample numbers.

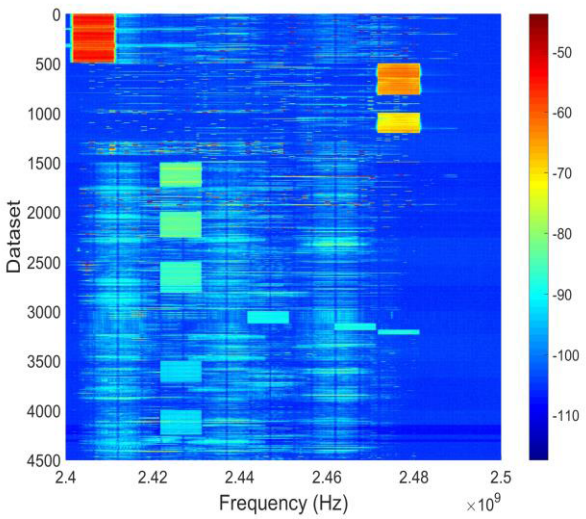

FIGURE 10. Training data for the outdoor environment.

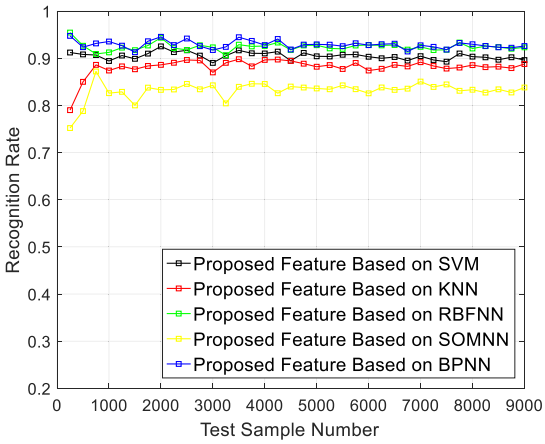

FIGURE 11. Recognition rate in an outdoor environment for different modeling methods and number of samples.

as a type of ANN is more suitable for UAV detection in indoor environment compared with other modeling methods.

When test sample number is 1500, the FAR are 0.1683, 0.20, 0.2676, and 0.0737 with the improved slope, skewness, kurtosis, and proposed feature based on ANN, respectively. While the FRR are 0.1372, 0.2307, 0.1669, and 0.07934 using above four ways in the distance of 10m. So, Figs. 7 and 8 obviously show that the proposed algorithm based on ANN provides the lowest error rate for non-UAV and UAV signal in the indoor environment. With the same number of samples, the FRR of proposed feature are 0.0655, 0.0809, and 0.0967 at the indoor distance of 5 m, 10 m, and 15 m. Besides, the recognition rate of proposed feature based on ANN are 0.9267, 0.8952, and 0.8786 at the distance of 5 m, 10 m, and 15 m respectively. So, the FRR and the recognition rate will decrease along with the increase of distance. In Fig. 6, Fig. 7, Fig. 8, and Fig. 9, the result changes a lot from samples number 250 to 500 owing to the un-stability of a small amount of sample. Furthermore, the FAR, FRR and recognition rate tend to be stable with the increase of test sample number.

B. OUTDOOR UAV TEST

Part of outdoor received data is used for training as shown in Fig. 10 with datasets of 1 to 500, 501 to 1000, 1001 to 1500, 1501 to 2000, 2001 to 2500, 2501 to 3000, 3001 to 3500, 3501 to 4000, and 4001 to 4500 corresponding to a distance of 0.005 km, 0.01 km, 0.02 km, 0.5 km, 1 km, 1.5 km, 2 km, 2.5 km, and 3km between Rx and u. Obviously, the data of the front half for each distance belongs to the UAV class, while the data of the back half of signal for each distance belongs to the non-UAV class. After training, a modal is formed to detect the UAV signal.

Fig. 11 shows the recognition rate using five nonlinear modeling methods in an outdoor environment with a different number of random samples from 250 to 9000. The FAR of non-UAV class data using four techniques is given in Fig. 12 with the same sample numbers. While with the same sample numbers, the FRR of UAV class data is shown in Fig. 13 using four feature detection algorithms. Fig. 14 shows the recognizing UAV rate from different number of random data using proposed feature detection algorithm in an outdoor environment.

In Fig. 11, when the outdoor test sample number is 4250, the recognition rate of SVM, KNN, RBFNN, SOMNN and BPNN are 0.9106, 0.8828, 0.9252, 0.8459, and 0.9368 respectively. It is obvious that KNN and SOMNN have lower performance than other ways because of lazy learning method and forming dead neurons respectively. Besides, BPNN has better accuracy than SVM. Although the performance of BPNN is very similar to RBFNN, BPNN has a simpler structure than RBFNN. Therefore, BPNN we used as a type of ANN is more suitable for UAV detection in outdoor environment compared with other modeling methods.

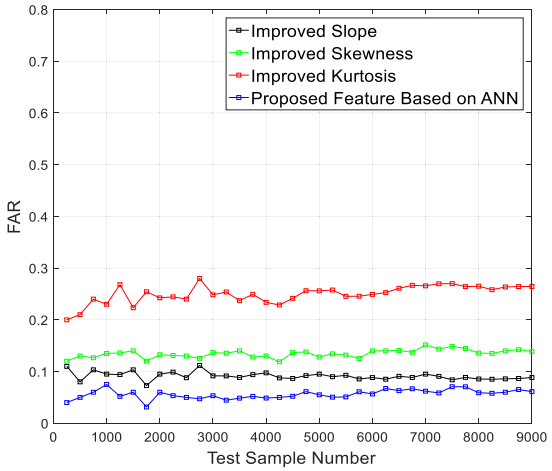

FIGURE 12. FAR with four feature detection algorithms in an outdoor environment.

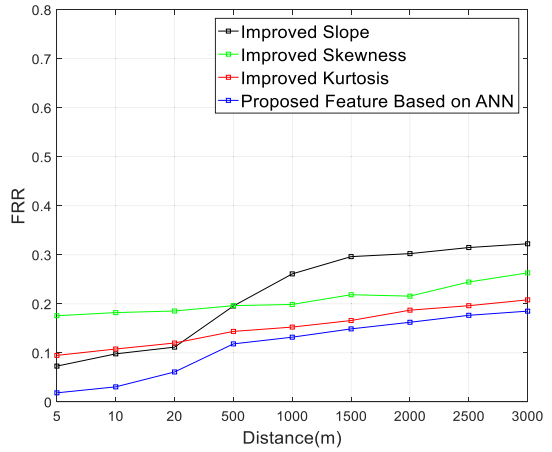

FIGURE 13. FRR with four feature detection methods in an outdoor environment for different distances with 4500 samples.

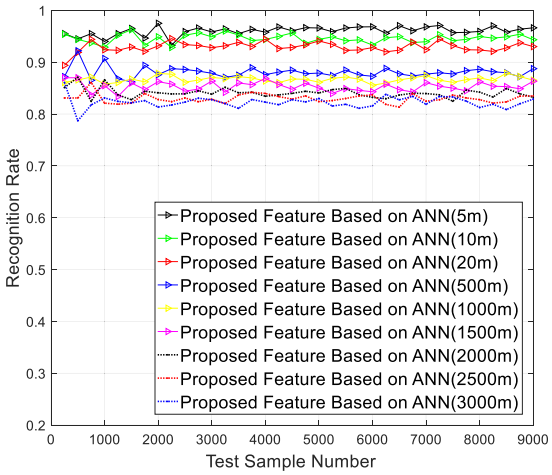

FIGURE 14. Recognition rate in an outdoor environment for different distances and number of samples.

When test sample number is 4500, the FAR are 0.0867, 0.1354, 0.2413, and 0.0522 with the improved slope, skewness, kurtosis, and proposed feature based on ANN, respectively. With the same number of samples, the FRR of four features above are 0.2612, 0.1989, 0.1527, and 0.1321 at the distance of 1000 m. Figs. 12 and 13 indicate that the proposed algorithm provides the lowest error rate for non-UAV and UAV signal compared with improved slope, skewness, and kurtosis detection in an outdoor environment. The recognition rate with the proposed algorithm are 0.9636, 0.9574, 0.9294, 0.8847, 0.8675, 0.8477, 0.8398, 0.8279, and 0.8257 for outdoor distances of 5 m, 10 m, 20 m, 500 m, 1000 m, 1500 m, 2000 m, 2500 m, and 3000 m, respectively. Fig. 14 shows that the recognition rate decreases with increasing distance. Further, the FAR and the recognition rate are approximately constant with an increase in the number of samples. The indoor UAV recognition rate is lower than the outdoor rate for the same distance because of the complexity of the indoor environment. The recognition rate is above 82% within a distance of 3 km.

VI. CONCLUSION

In this paper, an ANN detection algorithm for a UAV RF signal was proposed which employs three signal features of improved slope, improved skewness, and improved kurtosis. The classification of the UAV signal and the non-UAV signal was solved effectively. The FAR, FRR and recognition rate were analyzed for indoor and outdoor cases utilizing the data our collected. It was shown that the proposed algorithm based on ANN outperforms other recognition technologies of the improved slope, skewness, and kurtosis employed in the literature. Further, the recognition rate with the proposed solution decreases when the distance increases or the environment changes from outdoor to indoor. The error rate and the recognition rate tend to be stable with the increase of test sample number. Meanwhile, the recognition rate can maintain above 82% within the distance of 3 km, which is better than other UAV detection methods such as active radar, acoustic, and visual recognition.

REFERENCES

[1] L. Xu, J. Wang, H. Zhang, and T. A. Gulliver, "Performance analysis of IAF relaying mobile D2D cooperative networks," *J. Franklin Inst.*, vol. 354, no. 2, pp. 902–916, Jan. 2017.

[2] F. Luo *et al.*, "A distributed gateway selection algorithm for UAV networks," *IEEE Trans. Emerg. Topics Comput.*, vol. 3, no. 1, pp. 22–33, Mar. 2015.

[3] L. Xu, J. Wang, Y. Liu, W. Shi, and T. A. Gulliver, "Outage performance for IDF relaying mobile cooperative networks," *Mobile Netw. Appl.*, vol. 2017, no. 5, pp. 1–6, Dec. 2017.

[4] L. Xu and T. A. Gulliver, "Performance analysis for M2M video transmission cooperative networks using transmit antenna selection," *Multimed. Tools Appl.*, vol. 76, no. 22, pp. 23891–23902, 2017.

[5] C. Kanellakis and G. Nikolakopoulos, "Survey on Computer Vision for UAVs: Current Developments and Trends," *J. Intell. Robot. Syst.*, vol. 87, no. 1, pp. 141–168, Jan. 2017.

[6] Z. Liu, Z. Li, B. Liu, X. Fu, I. Raptis, and K. Ren, "Rise of mini-drones: Applications and issues," in *Proc. PAMCO*, Hangzhou, China, 2015, pp. 7–12.

[7] P. Nguyen, M. Ravindranatha, A. Nguyen, R. Han, and T. Vu, "Investigating cost-effective RF-based detection of drones," in *Proc. MobiSys*, Singapore, 2016, pp. 17–22.

[8] Y. Zhang and L. Yang, "Triangle and GA methods for UAVs jamming," *Math. Problems Eng.*, vol. 2014, pp. 1–8, Aug. 2014.

[9] C. Li and X. Wang, "Jamming of unmanned aerial vehicle with GPS/INS integrated navigation system based on trajectory cheating," *J. Nanjing Univ. Aeronaut Astronaut.*, vol. 49, no. 3, pp. 420–427, 2017.
[10] K. Hartmann and K. Giles, "UAV exploitation: A new domain for cyber power," in *Proc. CyCon*, Tallinn, Estonia, May 2016, pp. 205–221.
[11] D.-H. Shin, D.-H. Jung, D.-C. Kim, J.-W. Ham, and S.-O. Park, "A distributed FMCW radar system based on fiber-optic links for small drone detection," *IEEE Trans. Instrum. Meas.*, vol. 66, no. 2, pp. 340–347, Feb. 2017.
[12] R. May, Y. Steinheim, P. Kvaløy, R. Vang, and F. Hanssen, "Performance test and verification of an off-the-shelf automated avian radar tracking system," *Ecol. Evol.*, vol. 7, no. 15, pp. 5930–5938, Aug. 2017.
[13] J. Ren and X. Jiang, "Regularized 2-D complex-log spectral analysis and subspace reliability analysis of micro-Doppler signature for UAV detection," *Pattern Recognit.*, vol. 69, pp. 225–237, Sep. 2017.
[14] L. Xin and N. Xian, "Biological object recognition approach using space variant resolution and pigeon-inspired optimization for UAV," *Sci. China Technol. Sci.*, vol. 60, no. 10, pp. 1577–1584, Aug. 2017.
[15] E. E. Case, A. M. Zelnio, and B. D. Rigling, "Low-cost acoustic array for small UAV detection and tracking," in *Proc. NAECON*, Dayton, OH, USA, Jul. 2008, pp. 110–113.
[16] M. Foroutan and J. R. Zimbelman, "Semi-automatic mapping of linear-trending bedforms using 'self-organizing maps' algorithm," *Geomorphology*, vol. 293, pp. 156–166, Sep. 2017.
[17] M. Lopez-Ramirez, L. Ledesma-Carrillo, E. Cabal-Yepez, C. Rodriguez-Donate, H. Miranda-Vidales, and A. Garcia-Perez, "EMD-based feature extraction for power quality disturbance classification using moments," *Energies*, vol. 9, no. 7, p. 565, Jul. 2016.
[18] A. Zafar and K.-S. Hong, "Detection and classification of three-class initial dips from prefrontal cortex," *Biomed. Opt. Exp.*, vol. 8, no. 1, pp. 367–383, Jan. 2017.
[19] X. Liang, H. Zhang, T. Lu, and T. A. Gulliver, "Energy detector based TOA estimation for MMW systems using machine learning," *Telecommun. Syst.*, vol. 64, no. 2, pp. 417–427, Feb. 2017.
[20] X. Liang, H. Zhang, T. A. Gulliver, G. Fang, and S. Ye, "An improved algorithm for through-wall target detection using ultra-wideband impulse radar," *IEEE Access*, vol. 5, pp. 22101–22118, 2017.
[21] Y. Ding, Y. Wang, and D. Zhou, "Mortality prediction for ICU patients combining just-in-time learning and extreme learning machine," *Neurocomputing*, vol. 281, pp. 12–19, Nov. 2017.
[22] C. Hou, F. Nie, C. Zhang, D. Yi, and Y. Wu, "Multiple rank multi-linear SVM for matrix data classification," *Pattern Recognit.*, vol. 47, no. 1, pp. 454–469, 2014.
[23] Y. Wang, D. Zhao, Y. Li, and S. X. Ding, "Unbiased minimum variance fault and state estimation for linear discrete time-varying two-dimensional systems," *IEEE Trans. Autom. Control*, vol. 62, no. 10, pp. 5463–5469, Oct. 2017.
[24] X. L. Liang, H. Zhang, and T. A. Gulliver, "Energy detector based time of arrival estimation using a neural network with millimeter wave signals," *KSII Trans. Internet Inf. Syst.*, vol. 10, no. 7, pp. 3050–3065, Jul. 2016.
[25] S. Hengy *et al.*, "Multimodal UAV detection: Study of various intrusion scenarios," in *Proc. SPIE*, Warsaw, Poland, vol. 10434. Oct. 2017, p. 104340P.
[26] W.-C. Liu, T.-C. Wei, Y.-S. Huang, C.-D. Chan, and S.-J. Jou, "All-digital synchronization for SC/OFDM mode of IEEE 802.15.3c and IEEE 802.11ad," *IEEE Trans. Circuits Syst. I, Reg. Papers*, vol. 62, no. 2, pp. 545–553, Feb. 2015.
[27] X. Liang, H. Zhang, S. Ye, G. Fang, and T. A. Gulliver, "Improved denoising method for through-wall vital sign detection using UWB impulse radar," *Digit. Signal Process.*, vol. 74, pp. 72–93, Mar. 2018.
[28] X. Liang, H. Zhang, T. Lyu, H. Xiao, and T. A. Gulliver, "A novel time of arrival estimation algorithm using an energy detector receiver in MMW systems," *EURASIP J. Adv. Signal Process.*, vol. 2017, no. 83, pp. 1–13, Dec. 2017.
[29] A. A. M. Zin, M. Saini, M. W. Mustafa, A. R. Sultanac, and R. Rahimuddin, "New algorithm for detection and fault classification on parallel transmission line using DWT and BPNN based on Clarke's transformation," *Neurocomputing*, vol. 168, pp. 983–993, Nov. 2015.
[30] P. Kanirajan and V. S. Kumar, "Power quality disturbance detection and classification using wavelet and RBFNN," *Appl. Soft. Comput.*, vol. 35, pp. 470–481, Oct. 2015.

HAO ZHANG (SM'13) was born in Jiangsu, China, in 1975. He received the B.S. degree in telecom engineering and industrial management from Shanghai Jiaotong University, China, in 1994, the M.B.A. degree from the New York Institute of Technology, New York, NY, USA, in 2001, and the Ph.D. degree in electrical engineering from the University of Victoria, Victoria, BC, Canada, in 2004. From 1994 to 1997, he was an Assistant President of ICO (China) Global Communications Company. He is currently a Professor with the Department of Electrical Engineering, Ocean University of China. He is also an Adjunct Professor with the University of Victoria. His research interests include wireless signals recognition, cooperative networks communications, ultra-wideband systems, MIMO wireless systems, and spread spectrum communications.

CONGHUI CAO was born in Shanxi, China, in 1992. She received the B.S. degree in communication engineering from Jianghan University, Wuhan, China, in 2014, and the M.S. degree in communication and information system from the Ocean University of China, Qingdao, China, in 2016, where she is currently pursuing the Ph.D. degree. Her research interests include cooperative networks communications and wireless signals recognition.

LINGWEI XU was born in Shandong, China, in 1987. He received the B.S. degree from the Department of Communication and Electronics, Qingdao Technological University, Qingdao, China, in 2011, and the M.S. degree in electronic and communication engineering and the Ph.D. degree in intelligent information and communication system from the Ocean University of China, Qingdao, in 2013 and 2016, respectively. Since 2016, he has been with the College of Information Science and Technology, Qingdao University of Science & Technology.

T. AARON GULLIVER (SM'96) received the Ph.D. degree in electrical engineering from the University of Victoria, Victoria, BC, Canada, in 1989. From 1989 to 1991, he was a Defence Scientist with Defence Research Establishment Ottawa, Ottawa, ON, Canada. He has held academic positions at Carleton University, Ottawa, and the University of Canterbury, Christchurch, New Zealand. He joined the University of Victoria in 1999, where he is currently a Professor with the Department of Electrical and Computer Engineering. His research interests include information theory and communication theory, algebraic coding theory, cryptography, construction of optimal codes, iterative coding, MIMO communications, space–time coding, and ultra-wideband communications. He is a member of the Association of Professional Engineers of Ontario, Canada. He became a fellow of the Engineering Institute of Canada in 2002 and the Canadian Academy of Engineering in 2012.